Structures 80 (2025) 109773

Contents lists available at ScienceDirect

Structures

journal homepage: www.elsevier.com/locate/structures

Training and validation of a machine learning model for seismic vulnerability of masonry buildings in aggregate and selection of key parameters

Silvia Pinasco [a,*], Sergio Lagomarsino [a], Luca Oneto [a], Andrea Coraddu [b], Serena Cattari [a]

[a] Department of Civil, Chemical, and Environmental Engineering (DICCA), University of Genoa, Via Montallegro 1, Genoa 16145, Italy
[b] University of Technology, Delft, the Netherlands

ARTICLE INFO

Keywords:
Buildings in aggregate
Historical centers
Vulnerability features
Machine learning
In-plane
Out-of-plane

ABSTRACT

The seismic vulnerability assessment of masonry buildings in aggregate, typical of historical centers, remains a critical and widely debated topic. The complexity of this issue, driven by numerous parameters and uncertainties, has left many challenges unresolved by traditional analysis methods. This study addresses the problem through an innovative approach, leveraging state-of-the-art Machine Learning (ML) techniques to analyze the small historical center of Casentino (AQ), significantly affected by the 2009 L'Aquila earthquake. The availability of highly detailed data on structural characteristics and damage enables the identification of correlations between multiple vulnerability parameters and in plane and out-of-plane damage mechanisms. From these correlations, a subset of key factors was identified as most relevant for interpreting seismic vulnerability while being easily obtainable through in-situ surveys, offering an efficient basis for large-scale risk assessments. The robustness of this subset was validated on a second case study, Visso (MC), by comparing ML-predicted damage to observed damage following the 2016–2017 Central Italy earthquake. The results highlight the potential of ML techniques to enhance seismic risk evaluation and streamline data collection processes for broader applications.

1. Introduction

Artificial intelligence (AI) is proving to be an efficient support to classical modeling techniques also in engineering applications. Compared to traditional methods, AI offers advantages to deal with complex problems in which many (eventually correlated) variables are involved, becoming less straighthood the physical interpretation. Machine Learning (ML) is a major subfield of AI and refers to the capability of computers to learn without being explicitly programmed. The first uses of ML programs in civil engineering date back to the late 1980s [1–6]. However, as [7] indicate, there are also numerous applications of ML techniques in the field of earthquake engineering. The main topic areas are: Seismic hazard analysis [8–10], Identification of the Structural System, Monitoring and Characterization of Exposure [11–18], Damage Detection [19–25] and Seismic Fragility Assessment [26–28]. The use of ML to support decision-making in post-earthquake scenarios has been the most common so far. Convolutional Neural Networks (CNNs) have often been used for earthquake damage classification due to their effectiveness in image recognition and classification [22,29,30]. Several studies indeed rely on visual data such as satellite images, earthquake damage images, and radar data to train and test ML models. In general, classification algorithms such as Random Forest Classification (RFC), Gradient Boosting Classification (GBC) and Extreme Gradient Boosting Classification (XGBC) have generally shown better performance compared to regression methods [31]. Many studies aim at classifying seismic damage (into categories such as no damage, slight damage, moderate damage, severe damage and collapse [19], or using traffic-light-based systems, i.e., no damage, medium damage, severe damage [32] and predicting building usability to also improve decisions during the emergency phase [15,21]. However these objectives sometimes face challenges related to data quality and regional variability, making adaptations necessary for application in different contexts. So far, an analysis of the literature shows that damage detection using ML techniques has been developed mainly by referring to portfolios consisting primarily of isolated buildings [23,24,32] or by considering only a limited number of basic building features such as the number of floors,

* Corresponding author.
E-mail addresses: silvia.pinasco@edu.unige.it (S. Pinasco), sergio.lagomarsino@unige.it (S. Lagomarsino), luca.oneto@unige.it (L. Oneto), a.coraddu@tudelft.nl (A. Coraddu), serena.cattari@unige.it (S. Cattari).

https://doi.org/10.1016/j.istruc.2025.109773
Received 18 March 2025; Received in revised form 30 May 2025; Accepted 18 July 2025
Available online 31 July 2025

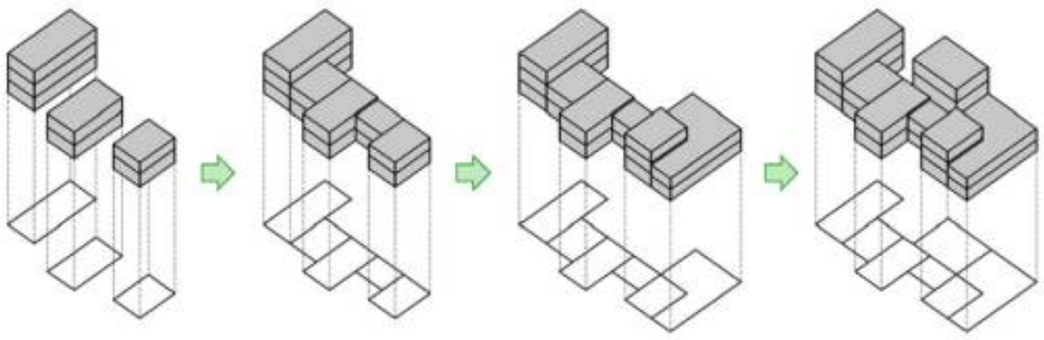

Fig. 1. Example of the historical evolution of a Building in Aggregate (BA).

construction period, height and floor area [25,32,33]. In this paper, the study focuses on the application of ML techniques for seismic damage assessment by referring to the typical built environment of small historical centers where masonry buildings are in aggregate configuration. Building in aggregate (BA) refers to a non-homogeneous set of structural units (SUs) interconnected with varying degrees of effectiveness determined by their evolutionary history, which may interact under seismic or dynamic actions [34], Fig. 1.

Assessing the seismic vulnerability of this type of building is very complex because, due to the historical evolution, it is characterized by a great variability in terms of materials, geometries, construction techniques, state of preservation, and types of connections between one SU and another [35]. As also discussed in [36], the seismic vulnerability of masonry aggregates is strongly influenced by the specific characteristics and historical development of the urban context in which they are located. Each historical center presents unique features in terms of urban morphology, construction practices, and transformation dynamics over time, which affect both the physical configuration of the aggregates and their structural behavior under seismic actions. These aspects are critical for understanding the vulnerability of such systems which led to adopt context-sensitive approaches in their assessment. An analysis of the state of the art reveals a lack of systematic and parametric analyses capable of addressing all the uncertainties and open issues that characterize this topic [37]. To date, numerous efforts and studies have been conducted in the literature to understand and investigate the seismic vulnerability of masonry buildings in aggregates, employing a wide range of methods, from mechanical models [38–41] to typological-heuristic approaches [42–45]. Notably, recent works have also focused on enhancing the automation of the assessment process [46,47]. However, given the complexity of the problem, many parameters come into play in assessing the seismic vulnerability of existing masonry BAs, and it is still unclear which of these are more important and what the correlations are among them.

For this purpose, the present work aims to determine a subset of parameters that best characterize the seismic vulnerability of BAs regarding both In-Plane (IP) and Out-Of-Plane (OOP) mechanisms, validating this subset of parameters on an additional case study. The ultimate goal is to establish a dedicated taxonomy for describing and characterizing the vulnerability of masonry BAs. This taxonomy is intended to serve as a systematic framework to identify and classify the parameters that most significantly influence the seismic response, enabling a more robust understanding of the interactions among them and providing a structured approach for future analyses based on either mechanical-analytical and mechanical-numerical approaches [37].

The structure of the paper consists of four main sections: a description of the methodology utilized, a presentation of the datasets used for training and validating the model, an explanation of the ML technique employed, and finally, a presentation of the results.

2. Methodological approach

The objectives of this work are to define a ML model with a good level of damage predictability and to determine and validate a subset of vulnerability parameters that are effective for damage prediction, while also being easily obtainable. This will allow for large-scale data collection in seismic risk policies during peacetime in future applications.

In many cases, especially in small historical centers, BAs have evolved spontaneously over the centuries without following specific rules or orders. This building process has resulted in a situation where, within this type of aggregates, it is often difficult to distinguish one SU from the adjacent ones, as they have a structural system that is strongly dependent on the rest of the aggregate, despite being legally considered independent SUs [37]. To address this difficulty, it was decided to operate by referring to three different scales, Fig. 2: the scale of the structural aggregate, the scale of the SU, and the scale of the single front. The problem of predicting seismic failure mechanisms in masonry aggregates was approached as a binary classification task using machine learning. Different feature sets describing building characteristics served as inputs to classify whether Out-Of-Plane or In-Plane mechanisms were activated. Several algorithms were tested, with XGBoost selected for its superior performance. The model was trained and validated through multiple scenarios to assess its ability to generalize to unseen data, including cross-site validation between different historical centers. Hyperparameter tuning and feature importance analysis ensured optimal and interpretable results. This approach provided a systematic and data-driven method to support seismic vulnerability assessment.

In the model's training phase, an initial dataset from the historical center of Casentino (AQ), affected by L'Aquila earthquake on April 6, 2009 (Mw=6.3), was considered to identify the correlations between damage mechanisms and vulnerability factors. The extensive data from this historical center was made available through site surveys conducted by the research units from the University of Genoa, the University of Catania, and the CNR-ITC of L'Aquila [48]. Using the ML technique the importance of features in relation to the considered damage mechanism was evaluated through the Mean Decrease Accuracy (MDA). Damage mechanisms were classified into IP and OOP modes. Specifically, the IP mechanisms Fig. 3*(a)* affect the response of walls when subjected to horizontal seismic actions oriented within their own plane, causing damage through flexure and shear [49,50]. The activation and propagation of cracks occurs when the ultimate material strength is exceeded. OOP mechanisms Fig. 3*(b)* instead involve rocking and bending phenomena that lead to structural collapse due to loss of equilibrium [51, 52] when walls are mainly subjected to horizontal seismic actions orthogonal to their main plan. These kinematic mechanisms can occur in buildings where the absence or ineffectiveness of connections between walls and floors, as well as between intersecting walls, does not ensure

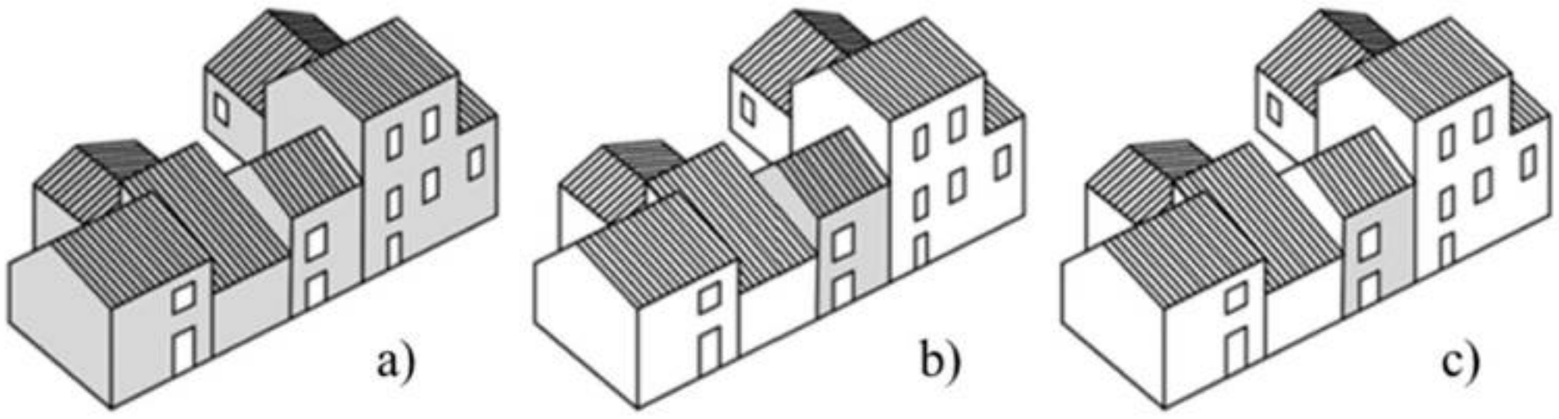

Fig. 2. Analysis scales referred to: a) aggregate scale, b) SU scale, c) front scale.

(a) (b) (c)

Fig. 3. Types of damage mechanisms: a) IP damage, b) OOP damage, c) damage from interaction between SUs.

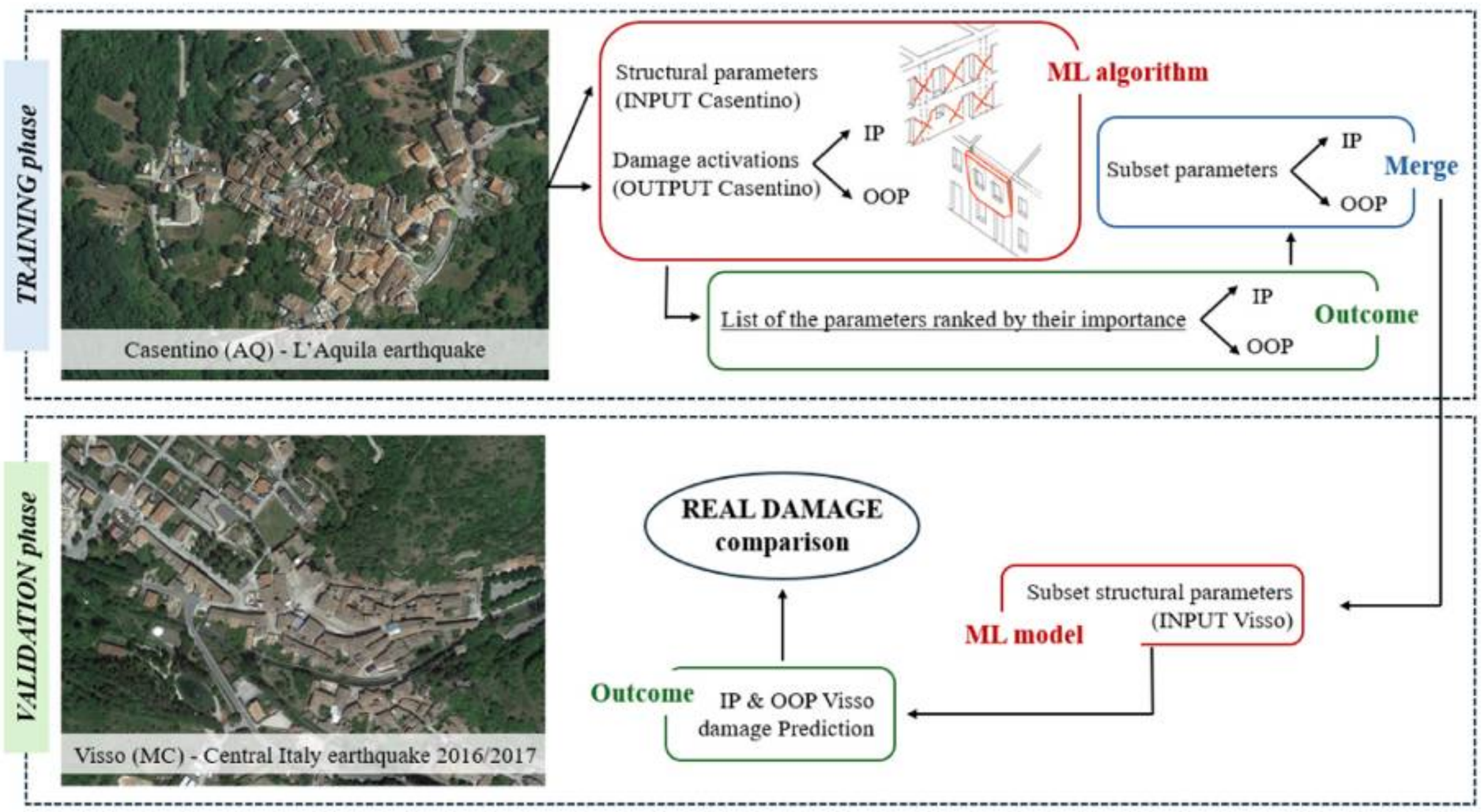

Fig. 4. Flowchart of the adopted methodology.

the development of an integrated structural behavior. In addition to IP and OOP damage modes, also pounding effect Fig. 3*(c)* may occur when adjacent SUs, due to their different oscillations during an earthquake, collide with each other [53,54].

Once the ranking of parameters based on their importance regarding the activation of both IP and OOP mechanisms was determined, the top 12 most important and easily obtainable parameters for IP and OOP were selected, and a merge of these was performed, resulting in a single subset of 15 parameters, that was then validated by referring to a second dataset from the historical center of Visso (MC). The Visso' municipality was subjected to the Central Italy 2016/2017 seismic sequence, where a damage prediction was made using ML. This prediction was subsequently compared with the actual recorded post-earthquake damage for the validation purpose, Fig. 4.

3. Dataset for training and validation of the model

In the context of seismic vulnerability assessment and damage prediction for historical BAs using ML techniques, the model's training and validation phases are crucial. To build a ML model it is essential to rely on a broad and representative dataset.

In this study, the historic center of Casentino (AQ) was used as the training model. The Casentino dataset includes detailed information on vulnerability parameters and structural characteristics of the buildings, collected through direct post-seismic inspections. This data is used to train the model, enabling the system to learn the relationship between structural features and observed damage.

Subsequently, to ensure that the trained model is robust and generalizable, it must be tested on independent data. For this purpose, the historic center of Visso (MC) was chosen as the validation model. Visso has similar architectural characteristics but with a distinct dataset compared to Casentino. Using this second model for validation tests the accuracy and reliability of the predictive model on new data, ensuring that the model's predictions are valid even in similar but not identical contexts.

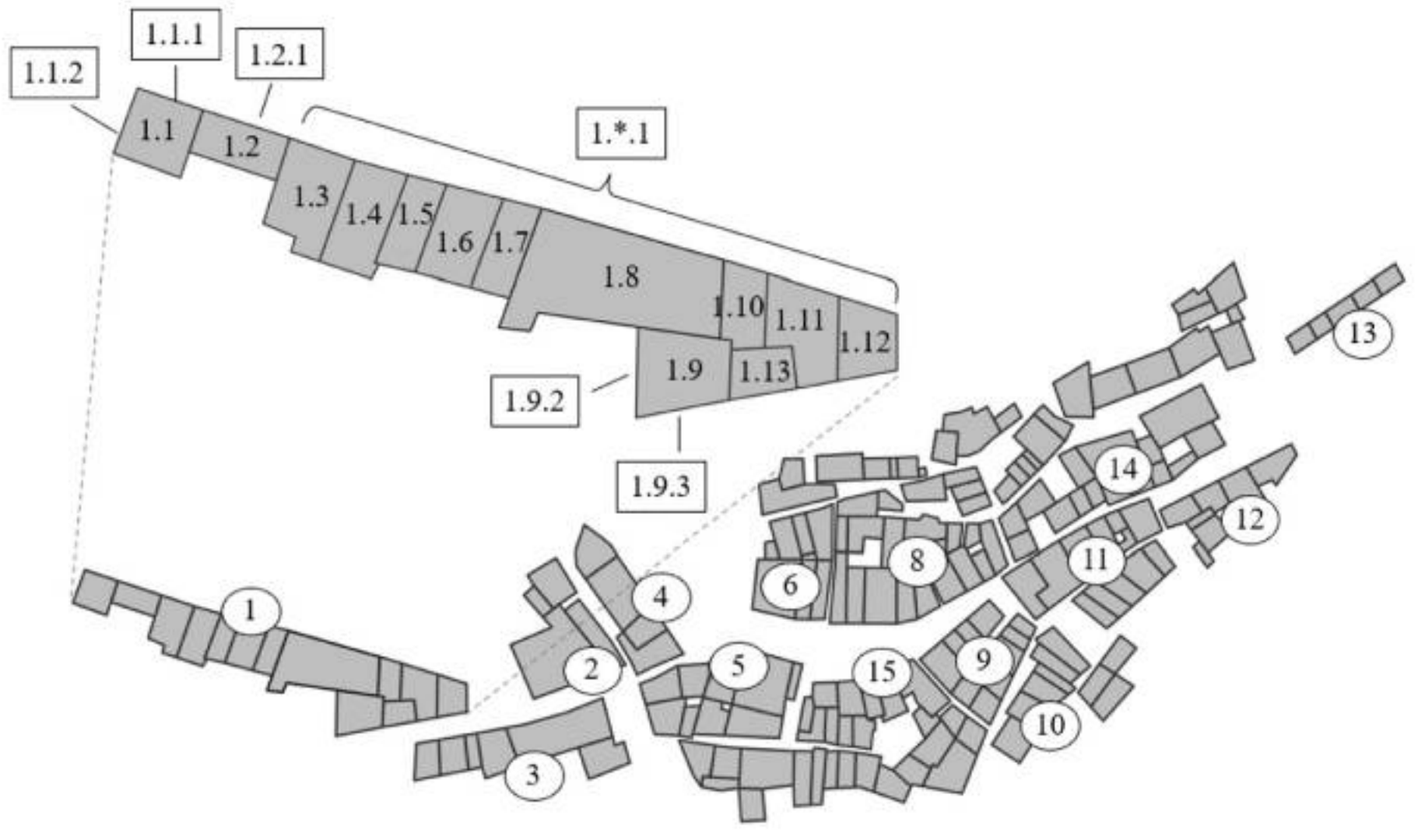

Fig. 5. Planimetric layout of the historic center of Visso. The numbers indicate the reference aggregate, the SUs that compose it, and the corresponding front.

3.1. Tools adopted for data collection

A crucial component of this study is the comprehensive data collection process, which forms the foundation for subsequent analysis and interpretation. The data necessary to train and validate the ML model can be categorized into two main groups: data related to structural and architectural details, which represent the input data in the analysis, and data related to damage, which represent the output data. This data were collected and classified with reference to the scale of the front Fig. 2. Starting from the base cartographic documentation (regional CTR 1:5000) integrated with data acquired from available aerial surveys, individual BAs, the SUs constituting them, and the fronts of each individual SU were identified and systematically classified to accurately map the association of each front with its respective SU and BA, Fig. 5. However, since the cartographic sources generally only outline the external boundaries of the aggregates, the identification of SUs required a more detailed operational approach. This process was carried out through extensive fieldwork conducted by a working group of researchers and students from the Universities of Genoa and Catania and researchers from ITC-CNR. The methodology included:

- Identification of the positions of walls orthogonal to the façades to reconstruct the internal planimetric configuration of the aggregate and to delineate the individual masonry cells;
- Survey of the number of floors along each façade to define the vertical consistency of the BA;
- Schematic documentation of all street-facing façades, highlighting cracks, collapses, tie rods, and other seismic protection elements, in order to capture the post-earthquake condition;
- Identification and classification of each SU based on construction techniques, damage patterns, and structural continuity.

The identification of BAs and their constituent SUs was thus the result of a mixed approach that combined cartographic analysis, systematic technological and structural surveys, and field experience. This integrated methodology was essential to understand the construction phases of the aggregates and to build a reliable and operationally useful dataset.

The identification of the SUs is a fundamental step not only to enable systematic data acquisition but also for a coherent interpretation of the damage. After this preliminary phase, it is important to highlight that the data collection process differed between the two historic centers. The data collection in the historic center of Casentino was carried out through post-earthquake field inspections conducted by a working group consisting of researchers and students from the Universities of Genoa and Catania and the researchers from ITC-CNR. These inspections carried out in the historic center of Casentino provided detailed information on the structural conditions and damage concerning 32 BAs, comprising a total of 256 SUs. Among these, 475 fronts were analyzed, resulting in a substantial amount of data. During these in-situ surveys, specific collection data forms were outlined and then compiled to account for the unique construction characteristics of Casentino [48,55]. This expedited data sheet for the survey of SUs within buildings in aggregate is provided in the supplementary material [56]. The form consists of two main sections. The first section includes information related to the general consistency of the SU, such as the position of the SU within the topographical context and the aggregate it belongs to, the general maintenance status, the total number of floors, etc., as well as more specific information on the construction survey of the individual

Fig. 6. Examples of damage in the historic center of Visso. Cracks IP are marked with X, while OOP activations are circled.

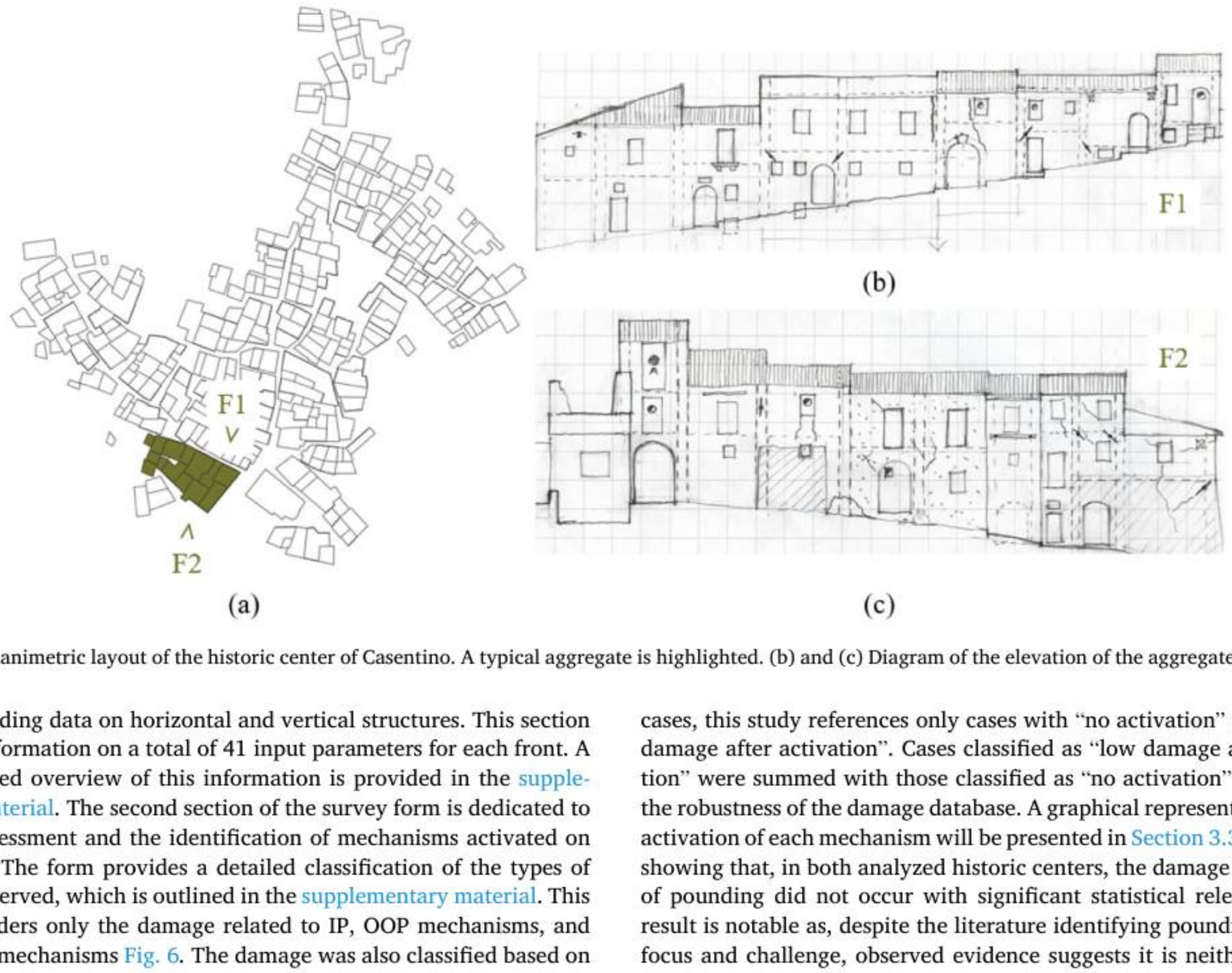

Fig. 7. (a) Planimetric layout of the historic center of Casentino. A typical aggregate is highlighted. (b) and (c) Diagram of the elevation of the aggregate highlighted.

fronts providing data on horizontal and vertical structures. This section provides information on a total of 41 input parameters for each front. A more detailed overview of this information is provided in the supplementary material. The second section of the survey form is dedicated to damage assessment and the identification of mechanisms activated on each front. The form provides a detailed classification of the types of damage observed, which is outlined in the supplementary material. This study considers only the damage related to IP, OOP mechanisms, and interaction mechanisms Fig. 6. The damage was also classified based on the activation level (no activation, low damage after activation, severe damage after activation). For IP damage mechanisms, the assignment of "low damage after activation" was applied in cases where the damage was localized to single panels of the analyzed front. Conversely, the assignment of "severe damage after activation" was given when shear of flexural damage to piers or spandrels was systematically distributed across at least one level of the building, Fig. 6. This approach reflects the equivalent frame model approach, where the wall is conceptualized as a system of piers and spandrels (deformable element where the non-linear response is concentrated) connected by rigid nodes which are not subjected to damage. In such systems, the distribution of damage in the masonry panels can activate different IP mechanisms, such as weak-story mechanisms (localized concentration of damage in a single story) or uniform mechanisms (damage distributed more evenly across multiple piers and spandrels).

These behaviors influence the residual properties of the structure, particularly its residual strength and displacement capacity, weak-story mechanisms, for example, tend to reduce the wall's overall displacement capacity due to the concentration of deformations, whereas uniform mechanisms often preserve a greater portion of both strength and ductility thanks to the more balanced distribution of damage. Similarly, the activation level was assigned for mechanisms related to OOP behavior. However, assigning a damage level to OOP mechanisms is complex because the observable damage often does not clearly or progressively reflect the severity of the phenomenon. Initial signs, such as microcracks or slight rotations, can be difficult to detect, especially if masked by plaster or hidden in hard-to-access areas. Unlike the distributed damage typical of IP mechanisms, OOP damage is often localized, such as edge overturning or the expulsion of limited portions of the wall, making it challenging to identify intermediate levels of deterioration. In summary, the observed damage can be subtle, localized, or difficult to interpret without an in-depth understanding of the structural context and support from more detailed analyses. In both cases, this study references only cases with "no activation" and "severe damage after activation". Cases classified as "low damage after activation" were summed with those classified as "no activation" to enhance the robustness of the damage database. A graphical representation of the activation of each mechanism will be presented in Section 3.3, in Fig. 13, showing that, in both analyzed historic centers, the damage mechanism of pounding did not occur with significant statistical relevance. This result is notable as, despite the literature identifying pounding as a key focus and challenge, observed evidence suggests it is neither frequent nor decisive, with its impact limited to localized masonry effects rather than the overall structural damage [57–59]. The data collected are derived not only from the notes on the survey forms but also from graphic sketches, annotations, and photographic documentation, Fig. 7.

This systematic data collection, useful for the purpose of this study, was originally carried out with the aim of acquiring elements for drafting a "Code of Practice" for repair interventions, seismic improvement, and reconstruction that could also support the municipal administration in making operational choices for reconstruction. While the data collected for the historic center of Casentino are extensive and detailed, those for the historic center of Visso were unfortunately obtained in a more expedited manner and partly through remote analysis. Specifically, 14 BAs were analyzed, comprising a total of 93 SUs, with 114 fronts examined. Information on structural parameters and damage was gathered by retrospectively analyzing photographs taken during post-earthquake field inspections conducted by the research team from the University of Genoa during the 2016–2017 earthquake sequence. This dataset included over 350 images of damage. The photographic material was further integrated with a detailed analysis of structural characteristics and damage using resources such as Google Street View, Google Earth, pre-earthquake YouTube videos, and videos recorded by firefighters immediately after the seismic event [60]. However, since the historic center of Visso is the case study used to validate the subset of parameters derived from the Casentino analysis, the number of parameters assigned to each front of the SUs of each BA is considerably lower than the number of parameters considered in Casentino. As one of the fundamental criteria for determining the subset of parameters is the ease of information retrieval, the attribution of parameters to the BAs of Visso was possible indirectly, without being on-site.

3.2. Historic center of Casentino (AQ)

The dataset used for ML training focuses on the historical center of

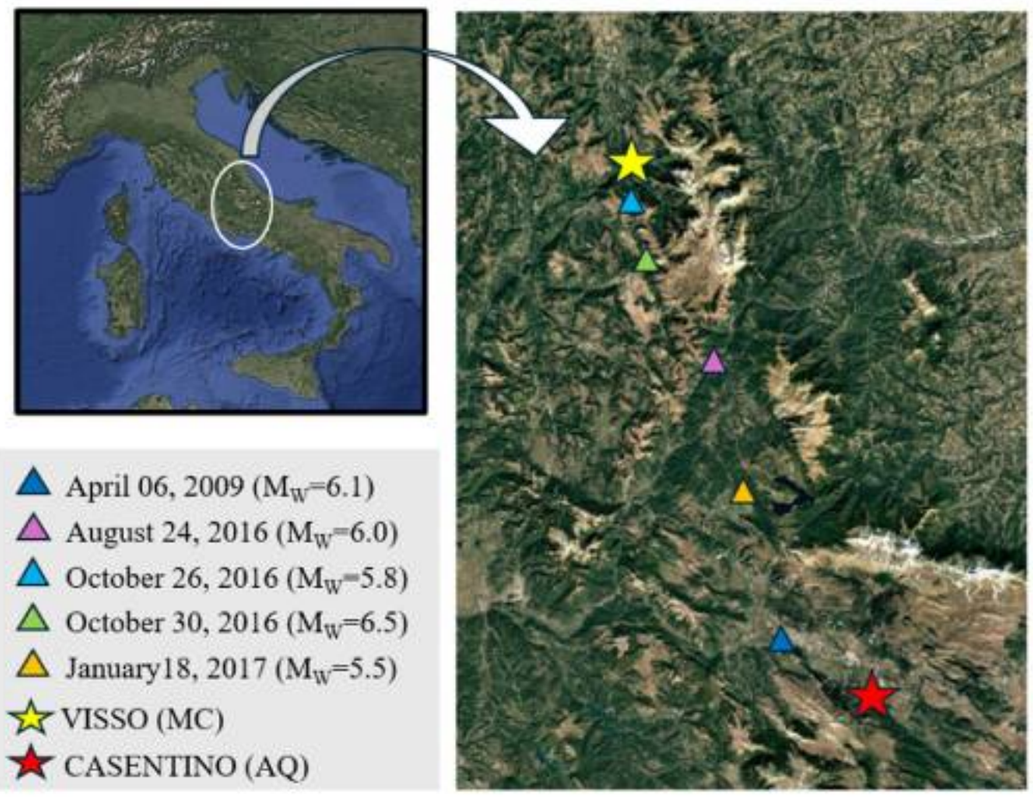

Fig. 8. Location of the historical centers under study and the earthquakes that affected them, https://www.earth.google.com.

Casentino (AQ), which was severely affected by the April 6, 2009, earthquake in L'Aquila. This earthquake occurred 2 km southwest of L'Aquila at a depth of 8.3 km, with a magnitude Mw= 6.3, Fig. 8. The epicenter was approximately 21 km from the historical center of Casentino, where the maximum PGA (Peak Ground Acceleration) experienced was estimated to be approximately 0.27 g, according to Shake Maps provided by the DaDo platform.

This case study was chosen because it is highly representative of the typical building fabric of small historical Italian centers and because a large amount of data is available for this area. Most of the buildings in the historic center of Casentino are in aggregate that have evolved over the centuries.

Despite the considerable variability in terms of materials, geometries, conservation status, and connections between adjacent SUs, it is possible to delineate some common characteristics across the entire building fabric. The buildings are primarily constructed from local sandstone, which is roughly shaped and bonded with sand-based mortar. Often, the mortar serves not only as a binder but also as a filling material. On average, the stone elements that comprise the structure are relatively small, with dimensions ranging from 15 to 30 cm. Vertical joints staggering is not consistently adhered to; however, there is a notable horizontal alignment of the courses. The floors are mainly made of wood, supported on a main beam perpendicular to the façade. Occasionally, steel floors and small vaults are present, particularly in buildings that have replaced existing floors or vaults. A recurring element in the building fabric of Casentino is the arch, which can be constructed from either local stone or brick. Arches are commonly found in openings and are also used as seismic reinforcement; numerous shoring arches are present throughout the area. Most SUs have two or three stories, and more than 60 % of the SUs lack any seismic protection devices, Fig. 9 and Fig. 10.

3.3. Historic center of Visso (MC)

The historic center of Visso (MC) was selected as a reference to validate the results obtained from the ML model, Fig. 11. Visso was significantly affected by the seismic sequence that struck Central Italy between 2016 and 2017. The main events of this seismic sequence that affected the area under examination are shown in Fig. 8. The most impactful event occurred on 30 October 2016, with an epicenter located 4 km north-west of Norcia (PG), at a depth of 10 km and a magnitude of 6.5. This earthquake was strongly felt in the historic center of Visso, located approximately 11 km from the epicenter, where the recorded PGA reached 0.39 g. This center was chosen due to its well-representative construction styles typical of central Italy. It primarily consists of masonry buildings (85 %), with the vast majority of these structures being in aggregate (93 %). The buildings in the historical center of Visso date back to the Middle Ages, with their construction periods primarily falling into two categories: pre 1919 and 1919–1945. The load-bearing walls of these structures are predominantly two-leaf stone masonry, featuring rough stones approximately 90–120 mm in height and 360–400 mm in length. The thickness of the external walls is around 70–80 cm on the ground floor and 55–60 cm on the upper floors. Internal walls tend to be somewhat thinner, typically 5 cm less than the perimeter walls on each floor.

There is a notable difference in the ratio of the total resistant wall section to the total surface when comparing the longitudinal and transversal directions. The transversal direction, often with side walls, exhibits a higher ratio, whereas fronts are oriented along the longitudinal direction, which runs parallel to the main axis of the BA. In

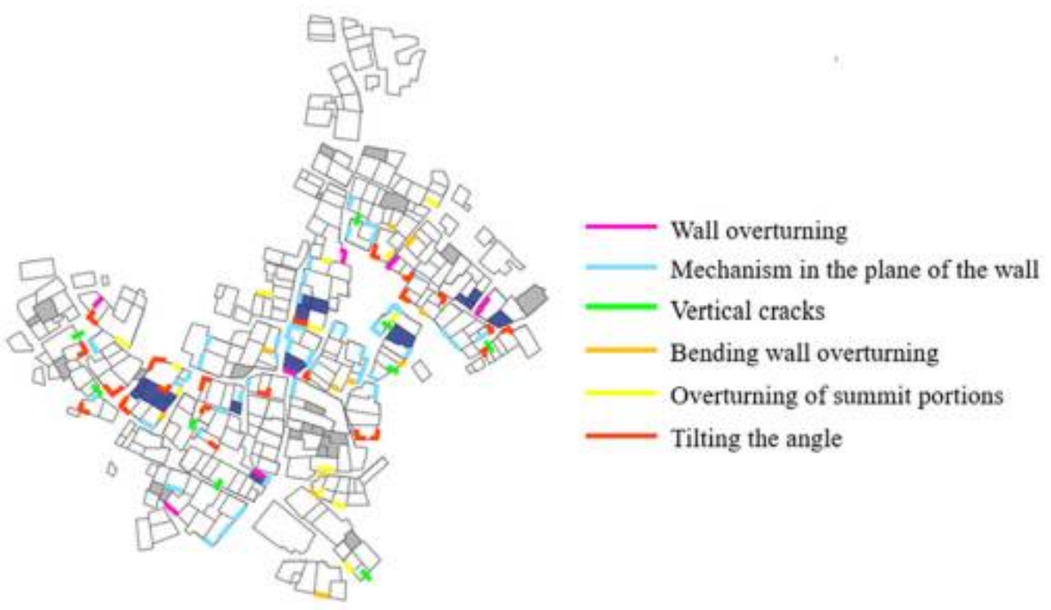

Fig. 10. Graphical representation of the damage mechanisms activated in the historic center of Casentino.

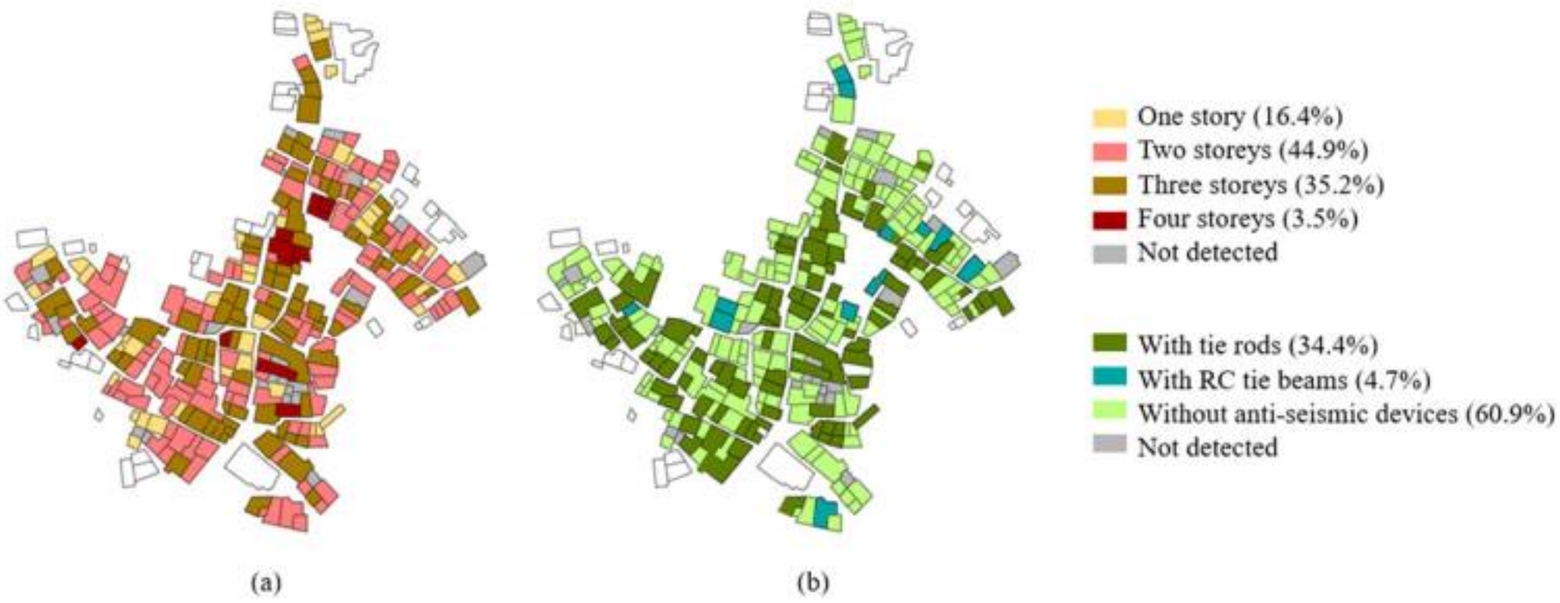

Fig. 9. Graphical representation of some building features in the historic center of Casentino: a) number of floors, b) anti-seismic measures.

Fig. 11. Planimetric and photographic representation of the damage of the historic center of Visso.

contrast, fronts oriented along the longitudinal direction are characterized by quite large openings at ground level. Floor diaphragms are predominantly made of brick and timber, though some cases include very thin, unreinforced concrete slabs, approximately 15 cm thick. The diaphragms are generally oriented perpendicular to the transversal direction [60].

A brief graphical summary of some of the collected data is presented Fig. 12 which also includes a comparison of the same parameters related to the historic center of Casentino.

Fig. 12 highlights the main structural differences and similarities between the two historical centers under study. In Casentino, buildings predominantly have three floors (46 %), though there is also a significant presence of two stories (31 %) and single-story buildings (18 %). In contrast, most SUs in Visso consist of two floors (65 %). In terms of topographic conditions, buildings in Casentino are mainly located on sloped ground (89 %), while in Visso, they are positioned on the flat terrain, indicating a notable difference in geographical setting between the two historical centers. In both villages, roofs are primarily constructed from wood, and SUs generally do not tower above their adjacent units. The arrangement of openings is predominantly regular, with 69 % of buildings in Casentino and 61 % in Visso featuring a regular pattern. The quality of wall interlocking, which is essential for structural cohesion, is better in Visso, where 61 % of buildings exhibit good interlocking, compared to only 29 % in Casentino. Finally, tie-rods are more frequently found in Visso (50 %) than in Casentino, where they are present in only 30 % of cases. For further information, please refer to Fig. 12. The summary of the different feature sets to predict the IP and OOP activations is reported Table 1. The feature sets (FS) analyzed in this study are three, differing based on the number of factors included within each set. These subsets were defined with the specific goal of reducing the number of parameters required for the field surveys, while ensuring that the analysis relies on features that are easily obtainable in real-word conditions and strongly correlated with the interpretation of the seismic response. The first feature set (FS1) includes all the information extracted from the survey forms presented in the supplementary material, summarized into 38 parameters. It represents the most comprehensive dataset. The second feature set (FS2) is composed of 15 of the 38 parameters in FS1. These parameters were selected following the analyses conducted on Section 4, focusing on those most strongly correlated with damage mechanisms and easily measurable on-site. Specifically, the parameters most correlated with damage, 12 for IP mechanisms and 12 for OOP mechanisms, were combined into a single subset by considering the overlapping factors, resulting in FS2. The third feature set (FS3) was derived from FS2 by removing two parameters for which sufficient and reliable data were unavailable for the historical center of Visso. The comparison of damage mechanisms, including IP (In-Plane), OOP (Out-of-Plane), and pounding, observed in the two historic centers is illustrated in Fig. 13. From the analysis of these charts, it becomes evident that pounding is not statistically significant compared to the other mechanisms. This observation contrasts with findings in the state-of-the-art literature [61] which often emphasize pounding as one of the most studied and debated issues, possibly due to its complexity and the fact that it remains an unresolved aspect in many cases. Despite this, the evidence from the damage analysis suggests that

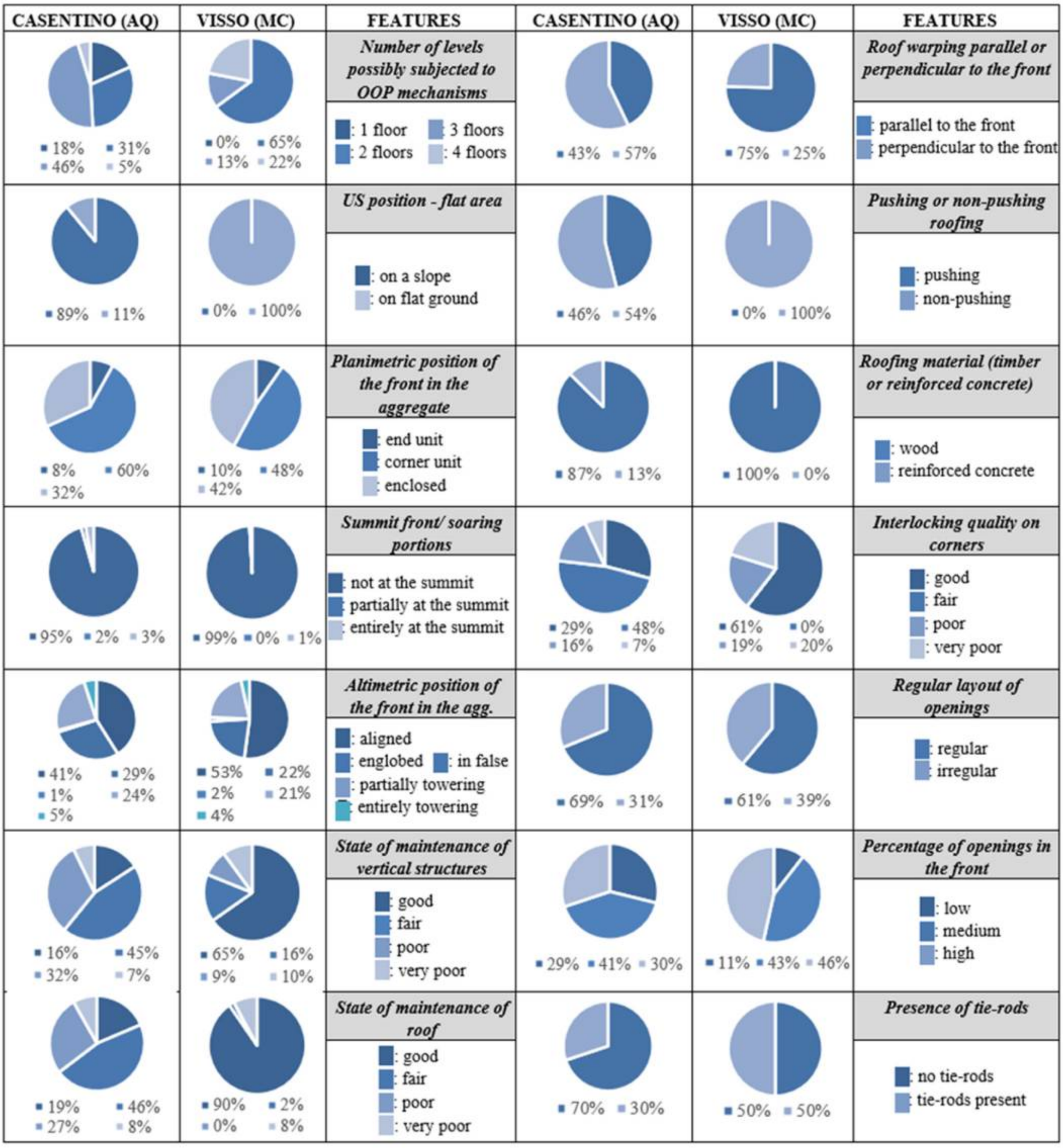

Fig. 12. Graphical summary of the structural features characterizing the historic centers of Visso and Casentino.

pounding is not among the most recurrent mechanisms. Furthermore, in the cases where pounding was observed, the analysis indicates that this type of damage does not appear to dominate the overall damage assessment of the structure. While pounding may have a localized effect on the response of specific masonry portions, it does not seem to be the decisive factor governing the overall response of the building unit.

4. Machine learning algorithm-based methodology

The problem described in Section 3 of predicting when an OOP or IP mechanism is activated based on the different feature set (FS1, FS2, and FS3) reported in Table 1, leveraging the data described in the very same section, can be mapped to a typical binary classification problem of ML [62]. In particular, in binary classification an input space $\mathscr{X}$ (i.e., the features sets of Table 1) and an output space (i.e., OOP or IP mechanism activation) $\mathscr{Y} \in \{-1, +1\}$ are available together with and unknown distribution $\mathbb{P}\{Y \mid X\}$ where $X \in \mathscr{X}$ and $Y \in \mathscr{Y}$.

The only knowledge about the $\mathbb{P}\{Y \mid X\}$ is a dataset of n observations $\mathscr{D}_n = \{(X_1, Y_1), \ldots, (X_n, Y_n)\}$, where $X_i \in \mathscr{X}$ and $Y_i \in \mathscr{Y}$ $\forall i \in \{1, \cdots, n\}$. An algorithm $\mathscr{A}_{\mathscr{H}} : \mathscr{D}_n \times \mathscr{F} \rightarrow f$ characterized by its hyperparameters $\mathscr{H}$ selects a model inside a set of possible ones $\mathscr{F}$ based on $\mathscr{D}_n$.

Two main types of algorithms exist (see Fig. 2). The error of $f =$

Table 1
Feature Sets.

Input/ Output	*Features Set*			*Description*
None	-	-	-	Historical Centre
	-	-	-	Aggregate
	-	-	-	Structural Unit
	-	-	-	Front
Input	FS1	FS2	FS3	Number of levels possibly subjected to OOP mechanisms
				SU position - flat area
				Grounding of the front in flat or slope area
				Position of the front in the aggregate (header, corner, internal)
				Front raised above a volume
				Position of the aggregate (aligned, encompassed, false, soaring)
				State of maintenance of vertical structures
				Roof warping parallel or perpendicular to the front
				Pushing or non-pushing roofing
				Roofing material (timber or reinforced concrete)
				Regular layout of openings
				Percentage of openings in the front
				Presence of tie-rods
			-	State of maintenance of the roof
			-	Interlocking quality corners
		-	-	Offset of diaphragms levels between adjacent SUs
		-	-	Front position in edge area
		-	-	Front position in subsidence area
		-	-	Levels number differentiated on adjacent fronts
		-	-	SU position - slope area
		-	-	Front advancement
		-	-	Presence of added volumes to the front
		-	-	Presence of raised-up portions
		-	-	Floor warping parallel or perpendicular to the front
		-	-	Presence of vaults
		-	-	Type of covering (flat/shallow)
		-	-	Presence of top ring-beam
		-	-	Maximum number of openings between two internal walls
		-	-	Presence of structural lintel
		-	-	Presence of wall thickening
		-	-	Presence of buttresses
		-	-	Presence of arches connecting two SUs
		-	-	Presence of ring-beams
		-	-	Connection with roofing elements
		-	-	Presence of adjacent but not interlocked walls
		-	-	Presence of infilled openings
		-	-	Presence of chimneys
		-	-	Presence of masonry portions inserted after previous collapses
Output	-	-	-	IP Activation ()
	-	-	-	OOP Activation ()

$\mathscr{A}_{\mathscr{H}}(\mathscr{D}_n) \in \mathscr{F}$ in approximating $\mathbb{P}\{Y \mid X\}$ is measured by a prescribed metric M. For what concerns the M many different metrics are available in literature [63]. In this work the percentage of balanced accuracy (PBACC), true positive (PTP), and true negative (PTN) are exploited. To tune the performance of the $\mathscr{A}_{\mathscr{H}}$, namely, to select the best set of hyperparameters, and to estimate the performance of the final model according to the desired metrics, a Model Selection (MS) and Error Estimation (EE) phase are performed [64]. The no-free-lunch theorem [65] ensures that to find the best algorithm and associated hyperparameters $\mathscr{A}_{\mathscr{H}}$ for a particular application, it is necessary to test multiple algorithms. In this case, four state-of-the-art algorithms for tabular data are tested [66,67]: Random Forests (RF) [68], XGBoost [69], Kernel Ridge Regression (KRR) [70], and the Extreme Learning Machine (ELM) [71] namely a Single Layered Neural Network [72] where the weights of the first layers have been randomly set reducing the computational burden of the training phase with minimal, if not absent, effect on accuracy. For space constraints, we will report just the results of the best performing algorithm: XGBoost. XGBoost [69] is a powerful supervised ML algorithm that excels in regression, classification, and ranking tasks. It is based on the boosting framework, where models are built sequentially to correct the errors of prior models, combining weak learners (typically decision trees) into a strong model. Using gradient descent optimization, it minimizes errors by focusing on residuals at each step. XGBoost incorporates regularization (L1 and L2) to prevent overfitting, efficiently handles missing values, and improves training speed with column subsampling and parallel processing. It assigns weights to harder or misclassified samples to refine predictions and uses tree pruning to limit model complexity. Supporting customizable loss functions and leveraging both first- and second-order derivatives, XGBoost is versatile, fast, and well-suited for structured/tabular data. For XGBoost, several key hyperparameters are tuned, including the learning rate of the gradient

l_r, the maximum depth of each tree n_d, the minimum loss reduction required for further partitioning

m_l, the number of training samples randomly selected for each tree's construction

n_b, and the number of features randomly sampled at each node n_f. Additionally, XGBoost effectively addresses class imbalance [73] in the data by adjusting the classification threshold t_h and the sampling percentage for each class p_c. A complete list of the hyperparameters tuned for XGBoost is provided in Table 2. The selection of the best hyperparameters depends on the specific scenario under consideration and on the metric exploited. It is possible to quantify and rank XGBoost's feature importance with a permutation test [74] that measures the mean decrease in accuracy: after the model is trained, you iterate through the columns of a held-out validation set, randomly shuffling one feature at a time while leaving the others intact; you then re-evaluate the model's accuracy (or any appropriate scoring function) on this permuted data. The drop in accuracy relative to the original baseline reflects how much the model relied on that feature: larger drops indicate more influential variables. Repeating the shuffle several times and averaging the losses yields a stable Mean Decrease in Accuracy score, which can be sorted to produce a feature-importance ranking that is model-agnostic, immune to internal tree heuristics, and directly tied to predictive performance.

Considering a single historical center (Casentino, which is the one with which we have enough data to train a model), three different and increasingly challenging extrapolating scenarios are studied, derived from the characteristics of the problem at hand. This approach allows an understanding of the extrapolation ability and robustness of the ML model:

- Leave one Front Out (LOFO): In this scenario, one Front is removed from the training set and kept it in the test set. The purpose of this scenario is to test the extrapolation ability of the model in terms of Fronts, namely, to estimate the model's ability to predict the URM damage of a Front never seen before;
- Leave one Structural Unit Out (LOUO): In this case, all the fronts of a SU are removed from the training set and kept in the test set. The purpose of this scenario is to test the extrapolation ability of the model in terms of SU, namely, to estimate the ability of the model to predict the URM damage of all the fronts of an SU never seen before;
- Leave one Aggregate Out (LOAO): Here, all the fronts of all the SUs of an Aggregate are removed from the training set and kept in the test set. The purpose of this scenario is to test the extrapolation ability of the model in terms of aggregate, namely, to estimate the ability of the model to predict the URM damage of all the fronts of an SU never seen before.

Additionally, another scenario, Leave One Historical Center Out (LOHCO), is considered, where the model is trained on the data from the

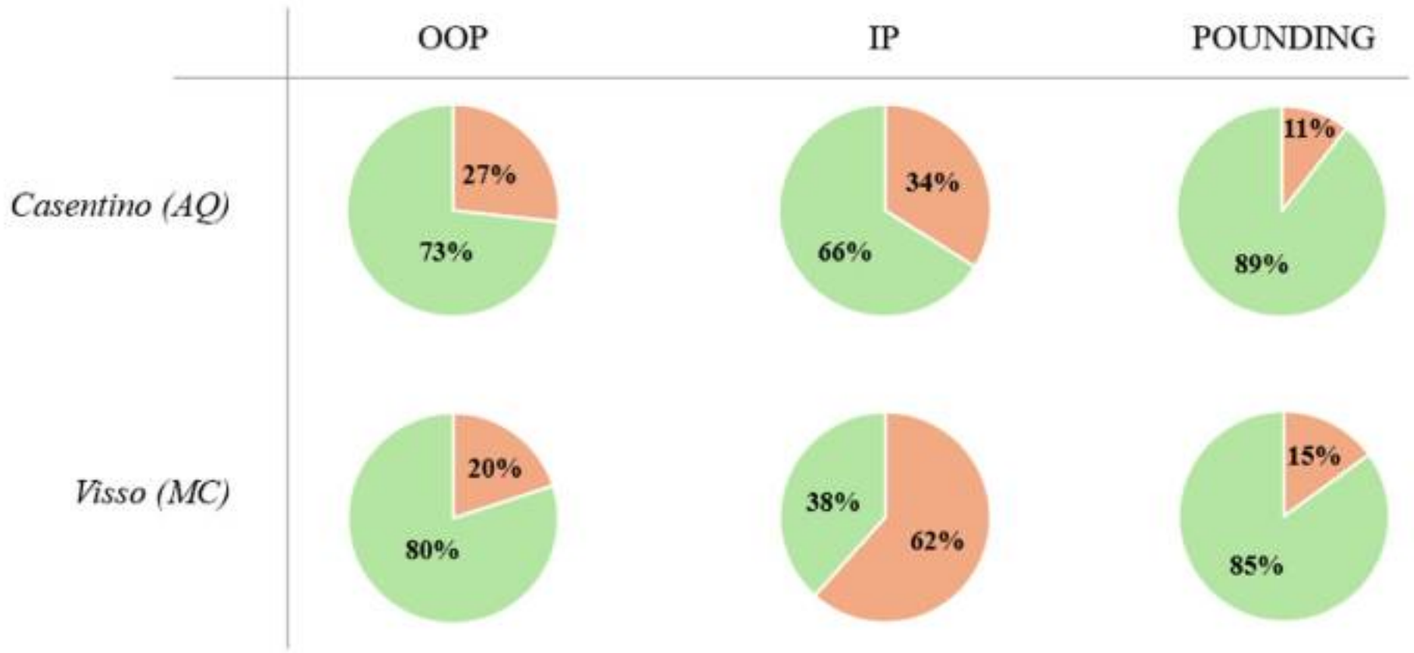

Fig. 13. Graphical representation of damage activations for IP, OOP and pounding in the historic centers of Visso and Casentino.

Table 2
Hyperparameters.

Algorithm	*Hyperparameters*
XGBoost	l_r: {0.01, 0.02, …, 0.005} n_d: {3, 5, 10} m_l: {0, 0.1, 0.2} n_b: {0.6, 0.8, 1}*n°samples n_f: {0.5, 0.8, 1}*n°samples t_h: {0.3, 0.35, …, 0.5} p_c: {0.95, 0.9, 0.85, 0.80}

Casentino historical center and then tested the model on Visso, another historical center. This scenario enables an assessment of how to tune the hyperparameters of the RF algorithm to generate the surrogate and evaluate its final performance [64].

For what concerns the last point, the answer is straightforward. Based on the different scenarios (LOFO, LOUO, and LOAO), we have to split the data in Training $\mathscr{D}_{\prime\prime}$ and Test $\mathscr{T}_{\prime}$ sets using the principle of the different extrapolating scenarios. For instance, in the LOUO scenario, all the fronts of a SU are placed in $\mathscr{T}_{\prime}$ while the remaining ones are kept in the $\mathscr{D}_{\prime\prime}$. The model is then trained on $\mathscr{D}_{\prime\prime}$ the best hyperparameters are selected, and the performance of the final model is assessed using $\mathscr{T}_{\prime}$. Repeating this procedure multiple times provides the average performance across different scenarios.

To tune the hyperparameters of the different ML algorithms, the following procedure is applied. First, $\mathscr{D}_{\prime\prime}$ is split into Learning $\mathscr{L}_{\prime}$ and Validation $\mathscr{V}_{\prime}$ sets, considering the same extrapolating scenario used for assessing the final performance. Then, each model is trained with $\mathscr{L}_{\prime}$ using various hyperparameter configurations, and its performance is measured on $\mathscr{V}_{\prime}$ according to the metric of interest. The experiment is repeated multiple times, and the hyperparameters configuration that yields the best PBACC on the validation sets is selected. Finally, the model is retrained with the selected best hyperparameters configuration on the entire $\mathscr{D}_{\prime\prime}$, resulting in the model used for testing purposes (see the previous paragraph).

5. Results

In this section we will report the results of applying the methodology described in Section 4 on the data described in Section 3.

Section 5.1 considers the Casentino historical center in the different scenarios (LOFO, LOUO, and LOAO) for both IP and OOP activations using the different feature set of Table 1 (FS1, FS2, and FS3). Section 5.2 considers the Visso historical center in the LOHCO scenario for both the IP and OOP activations using the different feature set of Table 1 (just FS2 and FS3 as FS1 is not available for Visso).

5.1. Outcomes from the algorithm trained on Casentino Historical Center

The data analysis reveals that the accuracy moving from the LOFO scenario to the LOAO scenario, considering all 38 input parameters (FS1), worsens but not significantly, for both IP and OOP mechanisms, as shown in Table 4. The values obtained indicate that the model's predictive capability is satisfactory. This demonstrates that the model is able to generalize well across different scenarios, maintaining robustness even when faced with increasingly challenging extrapolation scenarios. In Table 3, a list of input parameters is presented where the most important features in terms of the average accuracy of the expected result are displayed on the ordinate, from top to bottom. To further enhance the practical applicability of the model, a subset of parameters that are easily obtainable in the field during peacetime or post-earthquake assessments was selected (FS2, FS3). The top 12 parameters selected from the IP and OOP response lists are highlighted in blue. Among these, the parameters that are common to both lists are marked in bold blue, representing the shared factors that significantly influence both the IP and OOP behavior of the analyzed buildings, Table 3. A merge of these two sets was then performed, resulting in a refined subset of 15 input parameters. These parameters represent the most relevant structural characteristics for evaluating the vulnerability of BAs, offering a streamlined yet effective approach to damage prediction.

Importantly, the model's predictive accuracy, even with this reduced set of parameters, decreased by only 1 %, which is a negligible difference. The accuracy remains almost unchanged (reduction of less than 1 %) even when moving from FS2 to FS3, maintaining a good PBACC of around 71.9 ± 1.4 % for IP and 73.7 ± 2.2 % for OOP, Table 4. This minor drop in accuracy further underscores the efficiency and reliability of this reduced parameter selection for both IP and OOP mechanisms. The advantage of these subsets of parameters lies in its practicality: these parameters are not only sufficient to maintain high predictive accuracy but also easily accessible in field surveys, making them highly useful for future assessments and practical applications. This means that engineers and researchers can reliably use this smaller set of inputs to assess structural vulnerabilities without compromising the accuracy of their field surveys, leading to more efficient and faster evaluations, especially in post-disaster scenarios.

Regarding the interaction mechanisms between SUs, since the activation of these mechanisms was statistically underrepresented with the database, the ML model was unable to establish any meaningful correlation between this type of damage mechanism and structural features. This result highlights a potential area for future research, where increased data collection and more detailed analysis of SU interaction mechanisms could improve the model's ability to predict these types of damage more accurately. Therefore, the subset of selected parameters and the model's predictive accuracy are not only highly effective but also practical for future use, offering a balanced trade-off between

Table 3
Graphical representation of the vulnerability features ranked by importance from top to bottom according to the mean decrease accuracy for both IP and OOP mechanisms.

OOP	IP
State of maintenance of roof	**State of maintenance of vertical structures**
State of maintenance of vertical structures	**State of maintenance of roof**
Interlocking quality on corners	Presence of tie-rods
Pushing or non-pushing roofing	**Number of levels possibly subjected to OOP**
US position - flat area	Regular layout of openings
Grounding of the front in flat or slope area	Maximum number of openings between two internal walls
Floor warping parallel or perpendicular to the front	**Pushing or non-pushing roofing**
Number of levels possibly subjected to OOP	**Percentage of openings in the front**
Percentage of openings in the front	**US position - flat area**
Roof warping parallel or perpendicular to the front	**Front raised above a volume**
Position of the front in the aggregate (header, corner, internal)	Roofing material (timber or reinforced concrete)
Front raised above a volume	Position of the front in the aggregate (Aligned, encompassed, false, soaring)
US position - slope area	Presence of raised-up portions
Presence of tie-rods	Offset of diaphragms levels between adjacent USs
Levels number differentiated on adjacent fronts	Presence of structural lintel
Position of the front in the aggregate (Aligned, encompassed, false, soaring)	Levels number differentiated on adjacent fronts
Presence of raised-up portions	Presence of top ring-beam
Presence of structural lintel	Presence of chimneys
Presence of infilled openings	Roof warping parallel or perpendicular to the front
Regular layout of openings	Presence of added volumes to the front
Presence of wall thickening	Front advancement
Presence of vaults	Grounding of the front in flat or slope area
Presence of added volumes to the front	US position - slope area
Presence of masonry portions inserted after previous collapses	Presence of vaults
Connection with roofing elements	Presence of masonry portions inserted after previous collapses
Roofing material (timber or reinforced concrete)	Presence of adjacent but not interlocked walls
Presence of buttresses	Front position in subsidence area
Presence of adjacent but not interlocked walls	Presence of infilled openings
Front position in subsidence area	Type of covering (flat/shallow)

MEAN DECREASE ACCURACY

Table 4
Casentino Historical Center: ACC, FP, and FN for the LOFO, LOUO, and LOAO scenarios for both IP and OOP activations using the different feature set of Table 1 (FS1, FS2 and FS3).

Activation	*Scenario*	*PBACC*	*PTP*	*PTN*
FS1				
IP	LOFO	72.9 ± 1.4	72.3 ± 0.1	73.5 ± 2.7
	LOUO	72.0 ± 1.8	72.0 ± 1.7	72.1 ± 1.8
	LOAO	71.8 ± 1.7	71.2 ± 3.0	72.3 ± 0.4
OOP	LOFO	74.6 ± 2.8	74.6 ± 3.2	74.5 ± 2.4
	LOUO	73.3 ± 0.5	72.4 ± 0.4	74.2 ± 0.6
	LOAO	73.2 ± 2.1	73.0 ± 3.0	73.4 ± 1.2
FS2				
IP	LOFO	72.3 ± 1.2	71.3 ± 0.3	73.3 ± 2.2
	LOUO	71.6 ± 2.4	70.8 ± 1.7	72.4 ± 3.1
	LOAO	71.2 ± 2.8	70.9 ± 2.1	71.6 ± 3.4
OOP	LOFO	74.2 ± 2.1	74.2 ± 1.3	74.2 ± 3.0
	LOUO	73.2 ± 1.3	72.8 ± 1.3	73.5 ± 1.2
	LOAO	72.9 ± 2.9	71.9 ± 2.8	74.0 ± 2.9
FS3				
IP	LOFO	71.9 ± 1.4	71.6 ± 2.2	72.3 ± 0.6
	LOUO	70.9 ± 1. 3	70.9 ± 2.6	70.8 ± 0.1
	LOAO	70.9 ± 1.8	70.4 ± 1.1	71.4 ± 2.6
OOP	LOFO	73.7 ± 2.2	73.5 ± 1.5	73.9 ± 3.0
	LOUO	73.1 ± 2.4	72.6 ± 2.4	73.6 ± 2.4
	LOAO	72.4 ± 2.3	72.0 ± 1.2	72.8 ± 3.5

accuracy and field applicability. This makes the approach particularly suitable for real-time applications in both pre- and post-earthquake scenarios.

5.2. Validation results on the Visso historical center

To validate the obtained subset of parameters and assess its predictive capability on a case study not included in the training set, the robustness of the model and its ability to generalize predictions beyond the specific scenarios on which it was trained were analyzed. The results show that the model's ability to predict damage decreases by approximately 5 % for both subsets FS2 and FS3, reaching approximately 66.9

Table 5
Visso Historical Center: ACC, FP, and FN for the LOHCO scenario for both IP and OOP activations using the different feature sets FS2 and FS3 (as FS1 is not available for Visso).

Activation	**Scenario**	**PBACC**	**PTP**	**PTN**
FS2				
IP	LOHCO	66.9 ± 1.3	66.4 ± 0.1	67.5 ± 2.4
OOP	LOHCO	68.6 ± 1.7	68.5 ± 1.7	68.7 ± 1.7
FS3				
IP	LOHCO	72.3 ± 1.2	66.7 ± 2.8	67.8 ± 0.4
OOP	LOHCO	74.2 ± 2.1	69.1 ± 3.0	69.0 ± 2.2

Table 6
Legend of Table 7.

LEGEND	
	Parameter whose definition **fully** matches the one in the database and has been identified by the ML as **important**
	Parameter whose definition **fully** matches the one in the database and has been identified by the ML as **not important**.
	Parameter whose definition **partially** matches the one in the database, and for that match, the ML has identified it as **important**.
	Parameter whose definition **partially** matches the one in the database, and for that match, the ML has identified it as **not important**.
	Parameter **not included** in the database, for which the ML was therefore unable to provide an assessment.

± 1.3 % for IP mechanisms and 68.6 ± 1.7 % for OOP mechanisms in the case of FS2, and reaching approximately 67.3 ± 1.6 % for IP mechanisms and 69.1 ± 2.6 9 % for OOP mechanisms in the case of FS3, Table 5. This highlights the robustness of the model and its ability to generalize predictions beyond the specific training scenarios. These results are particularly noteworthy given the complexity of the topic and the fact that the model is predicting damage for a historical center, Visso, that was not used in the training process. This ability to generalize represents an excellent starting point, especially considering that the two feature sets, FS2 and FS3, are based on a limited number of parameters that are easily obtainable in the field, an element that enhances their practical applicability. A fundamental aspect to consider is that the damage observed in the historical centers of Casentino and Visso originated from different seismic events. During the damage assessment, the different seismic intensity levels affecting the two historical centers were considered, and in this case, no data re-centering operations were necessary. In Casentino, where the maximum recorded PGA was lower than in Visso, damage mechanisms were considered *not activated* only when the observed damage was DL0 (no damage). Conversely, in Visso, the *not activated* category also included cases with low levels of activation, while mechanisms were classified as *activated* only when the distribution or severity of damage was substantial (Fig. 6). This distinction reflects the fact that, although the vulnerability class was similar in both case studies, higher mean damage levels are associated with increasing intensity measure levels. According to this criterion, the damage classification adopted in the output database was solely based on the *activation/not activated* condition, ensuring consistency and robustness across both case studies. This approach allowed the model to maintain consistency and validity without introducing additional manipulations to the original data.

In the future, to further expand the applicability of the ML model and FS3, it will be necessary to systematically consider these aspects by integrating the initial database with new data from historical centers affected by varying seismic intensities. Such an expansion would allow the model to further improve its generalization capabilities and refine its predictions, making it an even more robust and effective tool for damage assessment in complex historical contexts.

5.3. Comparison of seismic vulnerability parameters ML-selected vs. score-based methods

To further validate the results obtained through ML, a comparison was carried out with vulnerability parameters proposed in score-based methods available in literature. Table 7 presents a comparison between the most significant parameters identified through ML analysis and those proposed by various Authors [43,44,75,76] for the application of score-based seismic vulnerability assessment methods. Parameters highlighted in dark green indicate a perfect match between those proposed by the Authors and those available in the analyzed database, which ML identified as particularly relevant for assessing the seismic vulnerability of buildings. Parameters highlighted in dark red indicate parameters whose definition fully matches that of the parameter analyzed in the database, but which the ML has identified as not essential for assessing seismic vulnerability. Conversely, parameters highlighted in light green represent only a partial match: in these cases, the definitions proposed by the authors encompass a broader and more detailed range of aspects compared to the individual parameters analyzed by ML. A significant example is parameter P1 from Formisano (Organization of vertical structures) and parameters P1 and P1.1 from Vicente and Stefanini (Type of resisting system), as well as parameters P1 and P3 from Brando (1st mode mechanism and 2nd mode mechanism), which, through their definitions, consider multiple specific aspects that characterize the building's resisting system as a whole, taking into account different possible sources of in-plane and out-of-plane fragility such as the presence of buttresses and/or iron ties, the quality of the connections with the transverse walls, or reinforced concrete ring beams with a transverse rigid diaphragm. In our database, however, the only available information was the presence or absence of tie rods, which was found to be highly relevant in the ML analyses. Therefore, to indicate the importance of the analyzed parameter while also highlighting its incomplete correspondence with the definitions provided by other Authors, it was decided to highlight the cell with a lighter shade of green. Another significant example is parameter P2 from Formisano (Nature of vertical distribution) and parameters P2 and P1.2 from Vicente and Stefanini (Quality of the resisting system), which include aspects such as masonry quality, considering material (size, shape, and type of stone), masonry texture, and quality of wall connections. However, due to the lack of information in the database, it was only possible to analyze the quality of connections, which ML identified as a highly significant parameter. For this reason, the Authors' parameters, which cover broader concepts, have been highlighted in light green, indicating a partial correspondence with those identified by ML. Another example includes parameters P3 from Formisano (Location of the building and type of foundation), P6 from Vicente (Location and soil condition), P13 from Brando (Site effects), and P3.1 from Stefanini (Building location and foundations). These definitions also account for the slope of the ground, a parameter that ML identified as important, but they additionally include information about the type of soil and foundations, which were not available in the analyzed database and, therefore, were not considered by ML. Finally, the cells highlighted in gray correspond to parameters that ML could not evaluate, not because they are irrelevant, but simply because they were not present in the database. This may be due to their absence in the survey form used, the difficulty in detecting them, or the fact that they were not relevant to the specific context of the analyzed historic center. In these cases, ML was unable to provide a judgment on their significance in the assessment of seismic vulnerability.

Conversely, the parameters proposed by the Authors whose definitions only partially match those of the parameters in the database and which the ML has identified as not important have been highlighted in light red. A significant example includes parameter P7 from Formisano (Type of floor), P11 from Vicente and P2.1 from Stefanini (Horizontal diaphragms), and finally P7 from Brando (Slabs). The definitions of

Table 7
Comparison between the parameters proposed in the literature for the application of score-based methods and the taxonomy derived from the ML analyses.

	FORMISANO ET AL.		VICENTE ET AL.		BRANDO ET AL.		STEFANINI ET AL.		Machine Learning
STRUCTURAL BUILDING SYSTEM	P1	Organization of vertical structures	P1	Type of resisting system	P1 P3	1st mode mechanism 2nd mode mechanism	P1.1	Type of resisting system	Presence of tie-rods
	P2	Nature of vertical structures	P2	Quality of the resisting system			P1.2	Quality of the resisting system	Interlocking quality corners
	P4	Distribution of plan resisting elements	P3	Conventional strength					
			P4	Maximum distance between walls			P1.5	Maximum distance between walls	
					P5	Arches	P3.4	Portico surfaces	
					P6	Vaults	/		
							P1.4	Maximum slenderness	
FLOOR SLABS AND ROOFS			P5	Numbers of floors	P2	Number of stories	P1.3	Numbers of floors	Number of levels possibly subjected to OOP mechanisms
	P7	Type of floor	P11	Horizontal diaphragms	P7	Slabs	P2.1	Horizontal diaphragms	
	P8	Roofing	P12	Roofing system	P8	Thrusting forces	P2.2	Roofing system	Pushing or non-pushing roofing Roof warping parallel or perpendicular to the front Roofing material (timber or reinforced concrete)
OPENINGS	P15	Percentage difference of opening areas among adjacent facade							
			P10	Wall facade openings and alignments			P3.5	Area of openings and alignments	Percentage of openings in the front Regular layout of openings
IRREGULARITIES	P5	Plan regularity	P8	Plan configuration	P11	Irregularities	P3.3	Plan configuration	
	P6	Height regularity	P9	Regularity in height			P3.7	Turrets	
INTERACTION	P12	Position of the building in the aggregate	P7	Aggregate position and interaction	P1	Position in the cluster	P16	Planimetric interaction	Position of the front in the aggregate (header, corner, internal)
	P14	Effect of either structural or typological heterogeneity among adjacent structural unit					P4.3	Typological and structural discontinuity	
	P11	Presence of adjacent buildings with different height					P4.1	Altimetric interaction	Position of the aggregate (aligned, encompassed, false, soaring) Front raised above a volume
	P13	Presence and number of staggered floors					P3.6	Presence of staggered floors	
					P14	Non seismic external hazard			
LOCATION	P3	Location of the building and type of foundation	P6	Location and soil conditions	P13	Site effects	P3.1	Building location and foundations	SU position -flat area Grounding of the front in flat or slope area
MAINTENANCE STATUS	P10	Physical conditions	P13	Fragilities and conservation state			P5.3	General state of conservation	State of maintenance of vertical structures State of maintenance of the roof
							P5.2	Interventions and changes to the original system	
NON-STRUCTURAL ELEMENTS	P9	Details	P14	Non-structural elements	P12	Non-structural elements	P5.1	Non-structural elements	
					P10	Stairs			
					P9	Presence of added structures	P3.2	Foreparts	

these parameters encompass a much broader range of aspects than those analyzed in the database, such as floor stiffness, the connections between the floor and the vertical seismic-resisting systems, the type of floor, the direction of the floor joists, deformations and support fragility. Among these, the only parameters recorded in the database and for which we had available information were the presence of vaults, the presence of tie beams, and floor warping relative to the main facade. However, these parameters were not found to be relevant in the ML analyses. It should be noted that some parameters, such as masonry quality and the type of floors, did not emerge as relevant in this study. This is because the two analyzed databases are relatively homogeneous in terms of masonry type and floor systems, resulting in a low data dispersion. Consequently, these parameters are less influential compared to others in assessing seismic vulnerability. However, the lack of relevance of these parameters does not undermine their well-established importance in the existing literature on masonry in general. The primary goal of this work was not to identify the key parameters for masonry buildings but to focus on BAs. The study highlighted the ability of ML to identify correlations between multiple vulnerability parameters and damage mechanisms, demonstrating excellent predictive capabilities. However, it is important to note that the analysis conducted cannot be considered conclusive for all vulnerability parameters, as some were not included in the analysis due to their absence or incompleteness in the survey sheets. In this study, the survey data were not altered; the decision was made to report and process the data without modifications to avoid the difficulty of reconstructing certain data and to prevent introducing an element of conventionality into the survey. Therefore, the parameters not analyzed, marked in gray in the survey sheets, represent an interesting area for future investigation. It is worth noting that, from a posteriori comparison, the parameters located in the cells colored in red, those identified as less influential by the ML, were found, in most cases, to have a lower weight in scoring methods, demonstrating a certain consistency between ML and scoring methods.

6. Conclusions

The integration of ML into civil engineering, particularly in the field of seismic damage assessment, has proven to be a transformative approach, providing valuable support to traditional methods. This study has demonstrated how ML can effectively address the complexities associated with assessing the seismic vulnerability of masonry buildings in historical centers, a task challenging by uncertainties related to variations in material, construction techniques, and the historical evolution of these structures. The application of ML techniques enabled the identification of subsets of parameters that better characterize building vulnerability with respect to both IP and OOP damage mechanisms. Through a rigorous methodology involving the comprehensive FS1 dataset from the historical center of Casentino, this research not only established a predictive model with satisfactory accuracy (approximately 72.9 ± 1.4 % for IP and 74.6 ± 2.8 % for OOP) but also highlighted the importance of parameter selection (FS2 and FS3). The identification of a refined subset of 12 parameters (FS3), which are both relevant and easily obtainable in the field, allows for a simplified approach to damage prediction, enhancing the practical applicability of the model in real-world scenarios. Results indicate that even with a reduced parameter set, the model's predictive accuracy experienced only a negligible decline, less than 1 % for FS2 and 1 % for FS3. This finding underscores the effectiveness of the parameter selection process, demonstrating that professionals can rely on the 12 input parameters of FS3 to maintain high accuracy in vulnerability assessments while significantly improving field survey efficiency. Validation of the model using a separate dataset from the historical center of Visso confirmed the robustness of the selected parameters (FS3). The model's ability to predict actual damage with an accuracy of 67.3 ± 1.6 % for IP and 69.1 ± 2.6 % for OOP reflects its capacity to generalize beyond the training set. This result is particularly significant given the inherent complexities associated with the data and the subjective nature of parameter attribution. The model's performance, therefore, is commendable, suggesting that it has effectively learned the underlying patterns associated with structural vulnerabilities despite the challenges posed by variability in data quality. To further validate the results obtained through ML, a comparison was carried out with vulnerability parameters proposed in score-based methods available in the literature. The analysis showed a strong correspondence between the most relevant parameters identified by ML and those traditionally considered significant in seismic vulnerability assessments. Moreover, the parameters identified as less influential by ML were generally found to have lower weights in traditional scoring methods, demonstrating a strong consistency between ML-based and conventional vulnerability assessment approaches. In summary, the findings of this study not only validate the applicability of the selected parameter subset but also reinforce the potential of ML models in enhancing real-time decision-making processes in both pre- and post-earthquake scenarios. By offering a balance between accuracy and field applicability, this approach can significantly improve seismic risk assessments in historical built environments. Future research could focus on expanding the dataset to include a greater number of parameters focused on interactions between SUs and analyzing how these interactions influence damage predictions. A deeper investigation of these parameters, considering boundary conditions such as the stiffness and resistance of adjacent SUs, could further improve ML models and enhance our understanding of seismic vulnerability in aggregated buildings. Such advancements would further enhance the model's predictive capabilities, providing even greater value in safeguarding these critical historical assets against seismic risks.

CRediT authorship contribution statement

Luca Oneto: Writing – original draft, Formal analysis, Software, Investigation. **Andrea Coraddu:** Software, Investigation, Writing – original draft, Conceptualization. **Serena Cattari:** Resources, Funding acquisition, Writing – review & editing, Project administration, Conceptualization, Supervision, Methodology. **Silvia Pinasco:** Validation, Methodology, Writing – original draft, Investigation, Data curation. **Sergio Lagomarsino:** Resources, Funding acquisition, Writing – review & editing, Project administration, Conceptualization, Supervision, Methodology.

Declaration of Competing Interest

The authors declare that they have no known competing financial interests or personal relationships that could have appeared to influence the work reported in this paper.

Acknowledgments

The study presented in the paper was developed within the research activities carried out in the frame of 2022–2024 and 2024–2026 ReLUIS Project– WP10 Masonry Structures (Coordinator– Prof. Guido Magenes). This project has been funded by the Italian Department of Civil Protection. The authors wish to thank Professor Caterina Carocci and her entire team (Department of Civil Engineering and Architecture (DICAR), University of Catania, SDS Syracuse, Italy) for their fieldwork, their preparation of the survey sheets, and the materials they shared with us. Note that the opinions and conclusions presented by the Authors do not necessarily reflect those of the funding entity.

Appendix A. Supporting information

Supplementary data associated with this article can be found in the online version at doi:10.1016/j.istruc.2025.109773.

References

[1] Arciszewski T, Mustafa M, Ziarko W. A methodology of design knowledge acquisition for use in learning expert systems. Int J Man Mach Stud 1987;27(1): 23–32. https://doi.org/10.1016/S0020-7373(87)80042-1.

[2] Ghaboussi XWJ, Garrett Jr JH. Knowledge-based modeling of material behavior with neural networks By J. Ghaboussi, 1 Member, ASCE, J. H. Garrett Jr., 2 Associate Member, ASCE, and X. Wu, 3 Student Member, ASCE. J Eng Mech 1991; 117(1):132–53. https://doi.org/10.1061/(ASCE)0733-9399(1991)117:1(132).

[3] Reich Y, Barai SV. Evaluating machine learning models for engineering problems. Artif Intell Eng 1999;13(3):257–72. https://doi.org/10.1016/S0954-1810(98)00021-1.

[4] Salehi H, Burgueño R. Emerging artificial intelligence methods in structural engineering. Eng Struct 2018;. 171(May):170–89. https://doi.org/10.1016/j.engstruct.2018.05.084.

[5] Stone JR, Blockley DI, Pilsworth BW. Towards machine learning from case histories. Civ Eng Syst 1989;6(3):129–35. https://doi.org/10.1080/02630258908970553.

[6] Reich Y. Machine learning techniques for civil engineering problems. ComputAided Civ Infrastruct Eng 1997;12(4):295–310. https://doi.org/10.1111/0885-9507.00065.

[7] Xie Y, Ebad Sichani M, Padgett JE, DesRoches R. The promise of implementing machine learning in earthquake engineering: a state-of-the-art review. Earthq Spectra 2020;36(4):1769–801. https://doi.org/10.1177/8755293020919419.

[8] Monterrubio-Velasco M, et al. A machine learning estimator trained on synthetic data for real-time earthquake ground-shaking predictions in Southern California. Commun Earth Environ 2024;. 5(1):1–11. https://doi.org/10.1038/s43247-024-01436-1.

[9] Mori F, et al. Ground motion prediction maps using seismic-microzonation data and machine learning. Nat Hazards Earth Syst Sci 2022;22(3):947–66. https://doi.org/10.5194/nhess-22-947-2022.

[10] Sun R, Qi W, Zheng T, Qi J. Explainable machine-learning predictions for peak ground acceleration. Appl Sci (Switz) 2023;13(7). https://doi.org/10.3390/app13074530.

[11] Giglioni V, Venanzi I, Ubertini F. A domain adaptation application for network-level post- earthquake damage classification. 18th Wolrd Conf Earthq Eng WCEE24 2024.

[12] Mori F, Spina D, Bocchi F, Mendicelli A, Naso G, Moscatelli M. Machine learning model for building seismic peak roof drift ratio assessment. Geomat Nat Hazards Risk 2023;14(1). https://doi.org/10.1080/19475705.2023.2182658.

[13] Pantoja-Rosero BG, Achanta R, Beyer K. Automated image-based generation of finite element models for masonry buildings. Bull Earthq Eng 2024;22(7):3441–69. https://doi.org/10.1007/s10518-023-01726-7.

[14] Salachoris GP, Standoli G, Betti M, Milani G, Clementi F. Evolutionary numerical model for cultural heritage structures via genetic algorithms: a case study in central Italy. Springe Neth 2024;22(7). https://doi.org/10.1007/s10518-023-01615-z.

[15] Tocchi G, Misra S, Padgett JE, Polese M, Di Ludovico M. The use of machine-learning methods for post-earthquake building usability assessment: a predictive model for seismic-risk impact analyses. Int J Disaster Risk Reduct 2023;97(June): 104033. https://doi.org/10.1016/j.ijdrr.2023.104033.

[16] Wang C, et al. Machine learning-based regional scale intelligent modeling of building information for natural hazard risk management. Autom Constr 2021;122 (December 2020). https://doi.org/10.1016/j.autcon.2020.103474.

[17] Xu Z, Wu Y, Qi M zhu, Zheng M, Xiong C, Lu X. Prediction of structural type for city-scale seismic damage simulation based on machine learning. Appl Sci (Switz) 2020;10(5). https://doi.org/10.3390/app10051795.

[18] Kutty AA, Wakjira TG, Kucukvar M, Abdella GM, Onat NC. Urban resilience and livability performance of European smart cities: a novel machine learning approach. J Clean Prod Dec. 2022;378. https://doi.org/10.1016/J.JCLEPRO.2022.134203.

[19] Abarquez JLB, Aquino DHM, Colegio KQ. Post-earthquake damage state classification using VGG-16 convolutional neural network. 18th World Conf Earthq Eng WCEE24d Conf Earthq Eng WCEE24 2024.

[20] Achmet Z, Diamantopoulos S, Fragiadakis M. Rapid seismic response prediction of rocking blocks using machine learning. Bull Earthq Eng 2024;22(7):3471–89. https://doi.org/10.1007/s10518-023-01680-4.

[21] Aloisio A, Rosso MM, Di Battista L, Quaranta G. Machine-learning-aided regional post-seismic usability prediction of buildings: 2016-2017 Central Italy earthquakes. J Build Eng 2024;91(March):109526. https://doi.org/10.1016/j.jobe.2024.109526.

[22] Bhatta S, Dang J. Hybrid Quantum-Classical Convolutional Neural Network for multiclass damage prediction of buildings. 18th World Conf Earthq Eng WCEE24 2024.

[23] Chen X, Zhang L, Lin X, Skalomenos KA, Chen Z. A clustering-based analysis method for simulating seismic damage of buildings in large cities. Eng Struct 2024; 307(29):117860. https://doi.org/10.1016/j.engstruct.2024.117860.

[24] Giardina G, et al. Combining remote sensing techniques and field surveys for post-earthquake reconnaissance missions. Bull Earthq Eng 2024;22(7):3415–39. https://doi.org/10.1007/s10518-023-01716-9.

[25] Mangalathu S, Sun H, Nweke CC, Yi Z, Burton HV. Classifying earthquake damage to buildings using machine learning. Earthq Spectra 2020;36(1):183–208. https://doi.org/10.1177/8755293019878137.

[26] Kalakonas P, Silva V. Earthquake scenarios for building portfolios using artificial neural networks: part I—ground motion modelling. Bull Earthq Eng 2024;22(7): 3655–76. https://doi.org/10.1007/s10518-022-01598-3.

[27] Pietro C, Marco D, Francesca da P. "Automatic identification of residential building features using machine learning techniques,". Procedia Struct Integr Jan. 2023;44: 1980–7. https://doi.org/10.1016/J.PROSTR.2023.01.253.

[28] Kalakonas P, Silva V. Earthquake scenarios for building portfolios using artificial neural networks: part II—damage and loss assessment. Bull Earthq Eng 2024;22(7): 3627–54. https://doi.org/10.1007/s10518-022-01599-2.

[29] Carpanese F, Donà P, Da Porto M. "Seismic risk assessment using machine learning for the automatic identification of building features. 18th World Conf Earthq Eng WCEE24 2024.

[30] Karimi N, Mishra M, Lourenço PB. Deep learning-based automated tile defect detection system for Portuguese cultural heritage buildings. J Cult Herit Jul. 2024; 68:86–98. https://doi.org/10.1016/j.culher.2024.05.009.

[31] Ghimire S, Guéguen P, Pothon A, Schorlemmer D. Testing machine learning models for heuristic building damage assessment applied to the Italian Database of Observed Damage (DaDO). Nat Hazards Earth Syst Sci 2023;23(10):3199–218. https://doi.org/10.5194/nhess-23-3199-2023.

[32] Ghimire S, Guéguen P, Giffard-Roisin S, Schorlemmer D. Testing machine learning models for seismic damage prediction at a regional scale using building-damage dataset compiled after the 2015 Gorkha Nepal earthquake. Earthq Spectra 2022;38 (4):2970–93. https://doi.org/10.1177/87552930221106495.

[33] Ghimire S, Guéguen P. Host-to-target region testing of machine learning models for seismic damage prediction in buildings. Nat Hazards 2024;120(5):4563–79. https://doi.org/10.1007/s11069-023-06394-z.

[34] ReLUIS, "Linee guida per il rilievo, l'analisi ed il progetto di interventi di riparazione e consolidamento sismico di edifici in muratura in aggregato - BOZZA 2010 in italian," 2010..

[35] Cima V, Tomei V, Grande E, Imbimbo M. The influence of the aggregate configuration on the seismic assessment of unreinforced masonry buildings in historic urban areas. Sustain 2024 Vol 16 Page 4172 May 2024;16(10):4172. https://doi.org/10.3390/SU16104172.

[36] Tosto C, Leggieri V, Ruggieri S, Uva G. A multisource methodology for the regional seismic fragility assessment of existing masonry buildings in historical centres. Int J Archit Herit Feb. 2025. https://doi.org/10.1080/15583058.2025.2461119;JOURNAL:JOURNAL:UARC20;REQUESTEDJOURNAL:JOURNAL:UARC20;WGROUP:STRING:PUBLICATION.

[37] Pinasco S, Lagomarsino S, Cattari S. Unreinforced Masonry Buildings in Aggregate of urban settlements: current approaches and critical issues for the Seismic Vulnerability Assessment. Structures 2024;73(February 2025):108335. https://doi.org/10.1016/j.istruc.2025.108335.

[38] Angiolilli M, Pinasco S, Cattari S, Lagomarsino S. On the vulnerability features of historical masonry buildings in aggregate. Procedia Struct Integr 2022;44: 2074–81. https://doi.org/10.1016/j.prostr.2023.01.265.

[39] Grillanda N, Valente M, Milani G, Chiozzi A, Tralli A. Advanced numerical strategies for seismic assessment of historical masonry aggregates. Eng Struct 2020; 212(March):110441. https://doi.org/10.1016/j.engstruct.2020.110441.

[40] Formisano A. Theoretical and Numerical Seismic Analysis of Masonry Building Aggregates: Case Studies in San Pio Delle Camere (L'Aquila, Italy). J Earthq Eng Feb. 2017;21(2):227–45. https://doi.org/10.1080/13632469.2016.1172376.

[41] Fagundes C, Bento R, Cattari S. On the seismic response of buildings in aggregate: Analysis of a typical masonry building from Azores. Structures 2017;10:184–96. https://doi.org/10.1016/j.istruc.2016.09.010.

[42] Vicente R, Parodi S, Lagomarsino S, Varum H, Silva JARM. Seismic vulnerability and risk assessment: case study of the historic city centre of Coimbra, Portugal. Bull Earthq Eng Aug. 2011;9(4):1067–96. https://doi.org/10.1007/S10518-010-9233-3.

[43] Formisano A, Florio G, Landolfo R, Mazzolani FM. Un metodo per la valutazione su larga scala della vulnerabilità sismica degli aggregati storici. XV Covegno ANDIS L'Ing sismica Ital 2011. (http://files/1292/Formisano_et_al_AGGREGATI.pdf).

[44] Brando G, De Matteis G, Spacone E. Predictive model for the seismic vulnerability assessment of small historic centres: application to the inner Abruzzi Region in Italy. Eng Struct 2017;153(September):81–96. https://doi.org/10.1016/j.engstruct.2017.10.013.

[45] Penna A, Rosti A, Rota M. Seismic response of masonry building aggregates in historic centres: observations, analyses and tests. Geotech Geol Earthq Eng 2022; 50:19–36. https://doi.org/10.1007/978-3-030-83221-6_2.

[46] Ruggieri S, et al. An archetype-based automated procedure to derive global-local seismic fragility of masonry building aggregates: META-FORMA-XL. Int J Disaster Risk Reduct Sep. 2023;95:103903. https://doi.org/10.1016/J.IJDRR.2023.103903.

[47] Leggieri V, Ruggieri S, Zagari G, Uva G. Appraising seismic vulnerability of masonry aggregates through an automated mechanical-typological approach. Autom Constr Dec. 2021;132:103972. https://doi.org/10.1016/J.AUTCON.2021.103972.

[48] Carocci C. Una metodologia per la conservazione di centri storici danneggiati dal sisma: rilievo costruttivo e del danno, indagini ed indicazioni per il recupero di Casentino (AQ). Sicur e Conserv nel Recuper dei beni Cult colpiti dal sisma Conf Ital 2010.

[49] Calderini C, Cattari S, Lagomarsino S. In-plane strength of unreinforced masonry piers. Earthq Eng Struct Dyn Jan. 2009;38(2):243–67. https://doi.org/10.1002/eqe.860.

[50] Celano T, Argiento LU, Ceroni F, Casapulla C. Literature review of the in-plane behavior of masonry walls: Theoretical vs. experimental results. Materials Jun. 2021;14(11):3063. https://doi.org/10.3390/ma14113063.

[51] Casapulla C, Giresini L, Lourenço PB. Rocking and kinematic approaches for rigid block analysis of masonry walls: state of the art and recent developments. Buildings Aug. 2017;7(3):69. https://doi.org/10.3390/buildings7030069.

[52] Abrams DP, AlShawa O, Lourenço PB, Sorrentino L. "Out-of-plane seismic response of unreinforced masonry walls: conceptual discussion, research needs, and modeling issues,". Int J Archit Herit 2017;11(1):22–30. https://doi.org/10.1080/15583058.2016.1238977.
[53] Bianchini N, et al. Influence of wall-to-floor connections and pounding on pre- and post-diction simulations of a masonry building aggregate tested on a shaking table. Bull Earthq Eng 2023;22(12):6141–61. https://doi.org/10.1007/s10518-023-01641-x.
[54] Malomo D, DeJong MJ. M-DEM simulation of seismic pounding between adjacent masonry structures. Bull Earthq Eng 2022;(ember). https://doi.org/10.1007/s10518-022-01545-2.
[55] Pinasco S, Cattari S, Lagomarsino S, Demšić M, Novak Š, Uros M. Numerical investigation of the seismic response of an unreinforced masonry residential buildings hit by Zagreb earthquake in 2020. Proc 2nd Croat Conf Earthq Eng 2CroCEE 2023.
[56] Carocci C. Small centres damaged by 2009 L'Aquila earthquake: On site analyses of historical masonry aggregates. Bull Earthq Eng Feb. 2012;10(1):45–71. https://doi.org/10.1007/S10518-011-9284-0.
[57] Z. Zhang, L. Davis, and D. Malomo, Simplified Assessment of the in-Plane Seismic Response of Old Brick Masonry Building Aggregates Using DE Macro-Crack Networks, 46. 2024. doi: 10.1007/978-3-031-39450-8_18..
[58] Wood P, Robins P, Hare J. Preliminary observations of the 2010 Darfield (Canterbury) earthquakes: an introduction. Bull NZ Soc Earthq Eng Dec. 2010;43(4):i–iv. https://doi.org/10.5459/bnzsee.43.4.i-iv.
[59] Miranda E, Bertero VV. Performance of low-rise buildings in Mexico City. Earthq Spectra Feb. 1989;5(1):121–43. https://doi.org/10.1193/1.1585515.
[60] Brunelli A, De Silva F, Cattari S. Observed and simulated urban-scale seismic damage of masonry buildings in aggregate on soft soil: The case of Visso hit by the 2016/2017 Central Italy earthquake. Int J Disaster Risk Reduct 2022;83:2212–4209. https://doi.org/10.1016/j.ijdrr.2022.103391.
[61] Pinasco S, Lagomarsino S, Cattari S. Unreinforced Masonry Buildings in Aggregate of urban settlements: current approaches and critical issues for the Seismic Vulnerability Assessment. Manuscr Submitt Publ 2024.
[62] Shalev-Shwartz S, Ben-David S. Understanding machine learning: From theory to algorithms. Underst Mach Learn Theory Algorithms Jan. 2013;9781107057:1–397. https://doi.org/10.1017/CBO9781107298019.
[63] Hossin M, Sulaiman MN. A Review On Evaluation Metrics For Data Classification Evaluations. Int J Data Min Knowl Manag Process Mar. 2015;5(2):01–11. https://doi.org/10.5121/IJDKP.2015.5201.
[64] L. Oneto, "Model selection and error estimation in a nutshell," 2020, Accessed: Oct. 08, 2024. [Online]. Available: ⟨https://link.springer.com/content/pdf/10.1007/978-3-030-24359-3.pdf⟩.
[65] Adam SP, Alexandropoulos SAN, Pardalos PM, Vrahatis MN. No free lunch theorem: a review. Springe Optim Appl 2019;145:57–82. https://doi.org/10.1007/978-3-030-12767-1_5.
[66] Fernández-Delgado M, Cernadas E, Barro S, Amorim D, Fernández-Delgado A. "Do we need hundreds of classifiers to solve real world classification problems?,". J Mach Learn Res 2014;15:3133–81. ⟨http://www.mathworks.es/products/neural-network⟩.
[67] Wainberg M, Alipanahi B, Frey BJ. Are random forests truly the best classifiers? J Mach Learn Res 2016;17:1–5. ⟨http://persoal.citius.usc.es/manuel.fernandez.delgado/papers/jmlr/data.tar.gz⟩.
[68] Breiman L. Random forests. Mach Learn Oct. 2001;45(1):5–32. https://doi.org/10.1023/A:1010933404324/METRICS.
[69] T. Chen and C. Guestrin, "XGBoost: A scalable tree boosting system," Proceedings of the ACM SIGKDD International Conference on Knowledge Discovery and Data Mining, 13-17-Augu, pp. 785–794, Aug. 2016, doi: 10.1145/2939672.2939785..
[70] Shawe-Taylor J, Cristianini N. Kernel methods for pattern analysis. Kernel Methods Pattern Anal Jun. 2004. https://doi.org/10.1017/CBO9780511809682.
[71] Huang GBin, Chen L, Siew CK. Universal approximation using incremental constructive feedforward networks with random hidden nodes. IEEE Trans Neural Netw Jul. 2006;17(4):879–92. https://doi.org/10.1109/TNN.2006.875977.
[72] Bishop CM, Bishop H. Deep Learning: foundations and Concepts. Deep Learn Found Concepts Jan. 2023:1–649. https://doi.org/10.1007/978-3-031-45468-4.
[73] Haixiang G, Yijing L, Shang J, Mingyun G, Yuanyue H, Bing G. Learning from class-imbalanced data: review of methods and applications. Expert Syst Appl May 2017;73:220–39. https://doi.org/10.1016/J.ESWA.2016.12.035.
[74] C. Molnar, Interpretable Machine Learning. Accessed: May 22, 2025. [Online]. Available: ⟨https://christophm.github.io/interpretable-ML-book/⟩.
[75] Ferreira TM, Vicente R, Mendes da Silva JAR, Varum H, Costa A. Seismic vulnerability assessment of historical urban centres: Case study of the old city centre in Seixal, Portugal. Bull Earthq Eng 2013;11(5):1753–73. https://doi.org/10.1007/s10518-013-9447-2.
[76] Stefanini S, Rovero L, Tonietti U. Seismic vulnerability assessment of historical masonry aggregate buildings. The case of Fes Medina in Morocco. Int J Archit Herit 2022;16(6):865–84. https://doi.org/10.1080/15583058.2021.1992537.